Physical Aging in Side-Chain Liquid Crystal Polymers: A DSC Investigation of the Enthalpy Relaxation

Laura Andreozzi,*,†,‡ Massimo Faetti,†,‡ Marco Giordano,†,‡ and Diego Palazzuoli†,‡

Department of Physics, University of Pisa, Via F. Buonarroti 2, I-56127 Pisa, Italy, and INFM UdR Pisa, Via F. Buonarroti 2, I-56127 Pisa, Italy

Received April 17, 2002; Revised Manuscript Received August 27, 2002

ABSTRACT: The enthalpy relaxation of the glasses of two side-chain liquid crystal polymethacrylates was studied with physical aging experiments detected with differential scanning calorimetry. The experimental traces were fairly well reproduced in the framework of a recent configurational entropic model. The temperature dependence of the equilibrium structural relaxation times was obtained with a simultaneous fit of several different thermograms and compared with the behavior found for the poly(methyl methacrylate) (PMMA). The comparison evidenced the stronger character of the two liquid crystal polymers, in the frame of the strong/fragile classification of glass-forming systems. At variance with the prediction of the energy landscape model, the heat capacity increment at the glass transition was greater than in PMMA, confirming some recent results on polymeric glass formers.

I. Introduction

Side-chain liquid crystal polymers have been greatly investigated in the past years,[1] also in virtue of their potential technological power. A representative example is found in liquid crystal polymers with functional mesogenic side-chain groups which contain azobenzene dye.[1,2] The photochemically induced change of the orientation of the azo molecules in the polymeric matrix provides a valuable mechanism[2−4] to obtain optical nanoscale writing and erasable storage of information.[3,5,6]

The stability properties of these optical memories may be affected by relaxation phenomena and diffusion processes, whereas the cooperative length of the system can influence the possibility of resolving the minimal bit. Consequently, the structural relaxation in the glassy state (or physical aging) is very important in determining the long-term performance of the system.

As a polymer is cooled through its glass transition, molecular mobility slows down until the material becomes a thermodynamically unstable glass, characterized by nonexponential and nonlinear character.[7] From this nonequilibrium glassy state, the system attempts to reach the equilibrium through the slow molecular configuration changes of the physical aging phenomenon.

Physical aging has been studied with many different experimental techniques.[8] Among them, differential scanning calorimetry (DSC) can detect the enthalpy relaxation of a glassy system. Phenomenological models have been proposed in order to describe this relaxation in polymers and glass-forming liquids.[7] Most of them are derived in the framework of the Tool−Narayanaswamy−Moynihan approach.[9,10] However, despite a general ability in reproducing experimental DSC scans, important discrepancies have been observed, especially in polymeric systems. A thermal history dependence has been evidenced for the model parameters,[7,11,12] which should only depend on the material; furthermore, the enthalpy lost during the isothermal annealing in glassy state may be significantly overestimated by the model predictions.[12,13] In a recent paper,[14] we confirmed the above trend for the enthalpy when DSC thermograms of an azo-side-chain liquid crystal (Azo-SCLC) polymethacrylate, were analyzed considering two different expressions of the instantaneous relaxation times.

In the present paper, we compare the enthalpy relaxation in that polymer and in a random copolymer synthesized starting from the monomeric unit of the Azo-SCLC polymethacrylate. Experimental data are treated in terms of a configurational entropy model,[15] which partially overcomes the mentioned difficulties.

II. Theoretical Section

The Tool−Narayanaswamy−Moynihan (TNM) approach[7] to the glass transition and its phenomenological assumptions will be briefly reviewed, before discussing the configurational entropy model.

The structural relaxation is depicted by the stretched exponential function[16]

$$\Phi(t) = \exp\left[-\left(\frac{t}{\tau}\right)^{\beta}\right] \tag{1}$$

with β ($0 < \beta \leq 1$) the stretching parameter, which describes the broadness of the spectrum of relaxation times of the system. β is retained independent of temperature by invoking the time−temperature superposition principle. τ is a characteristic time.

The structural state is considered by introducing a fictive temperature T_f,[9] which is the temperature at which the measured value of a property would be its equilibrium value. If the enthalpy H is taken as the relevant observable, T_f may be defined by[7]

$$H(T) = H_{eq}(T_f) - \int_T^{T_f} C_{p,glass}(\theta)\, d\theta \tag{2}$$

where $H_{eq}(T_f)$ is the equilibrium value of H at the temperature T_f and $C_{p,glass}(T)$ is the unrelaxed glassy heat capacity. On defining the fictive temperature, the

† University of Pisa.
‡ INFM UdR Pisa.
* Corresponding author: e-mail laura.andreozzi@df.unipi.it; tel ++39 050 2214000; fax ++39 050 2214333.

10.1021/ma020602y CCC: $22.00
Published on Web 10/22/2002

implicit assumption is employed for the *equilibrium* value of the enthalpy in the glass $dH_{eq}(T)/dT = C_{p,liq}(T)$.

Nonlinear effects are considered by assuming that the instantaneous relaxation rate depends on both the temperature and the glassy structure developed by the system during the aging process, so that $\tau = \tau(T_f,T)$.

By defining a reduced time and using the Boltzman superposition principle, one obtains[17]

$$T_f(T) = T_0 + \int_{T_0}^{T} dT' \left\{1 - \exp\left(-\left[\int_{T'}^{T} \frac{dT''}{Q\tau(T_f,T'')}\right]^{\beta}\right)\right\} \quad (3)$$

T_0 is a reference temperature well above the glass transition temperature and $Q = Q_{c,h}$ is the cooling/heating rate. Numerically integrating eq 3, the normalized $C_p^N = (dT_f/dT)$ may be evaluated and compared with the experimental value obtained by eq 2:

$$\frac{dT_f}{dT} = \frac{C_p(T) - C_{p,glass}(T)}{\Delta C_p(T_f)} \approx \frac{C_p(T) - C_{p,glass}(T)}{\Delta C_p(T)} \equiv C_p^N(T) \quad (4)$$

with

$$\Delta C_p(T) = C_{p,liq} - C_{p,glass} \quad (5)$$

$\Delta C_p(T)$ is the heat capacity increment between the glassy and liquid states, usually a very smooth function of temperature.

Among the models that define expressions for the instantaneous relaxation times, the Narayanaswamy−Moynihan (NM)[10,18] and the Sherer−Hodge (SH)[19]

$$\tau(T_f,T) = A \exp\left\{\frac{x\Delta h}{RT} + \frac{(1-x)\Delta h}{RT_f}\right\} \quad \text{NM} \quad (6)$$

$$\tau(T_f,T) = A \exp\left\{\frac{B}{RT(1 - T_2/T_f)}\right\} \quad \text{SH} \quad (7)$$

are considered qualitatively equivalent,[20] even if the SH model provides physically more realistic parameters and works better with the thermal history dependence of the parameters.[14,21] Indeed, the assumptions at the basis of the TNM models might be criticized,[22] and also the approach to nonlinearity could be inappropriate.[23] A suggestion that part of the difficulties[24] could be related to the definition of the equilibrated glass in terms of a thermodynamic extrapolation[12] comes from the enthalpy overestimation of TNM models in aging processes. In fact, major discrepancies are met in polymeric systems, where topological constraints could prevent the system from reaching the extrapolated equilibrium.

A different approach has been developed, where an equation for the evolution of the configurational entropy during physical aging is obtained. Adopting the configurational entropy as structure parameter provides the chance of considering the state of the system at very long times different from that extrapolated from the liquid or the rubber. The model is thoroughly described in recent papers;[15,22] accordingly, only the fundamental constitutive equations will be reported.

Let S_c be the configurational entropy of the system; the model proposes the evolution equation after a multiple-step thermal perturbation:

$$S_c(t) = S_c^{eq}(T_0) + \int_{T_0}^{T(t)} \frac{\Delta C_p^{lim}(\theta)}{\theta} d\theta - \sum_{i=1}^{n}\left(\int_{T_{i-1}}^{T_i} \frac{\Delta C_p^{lim}(\theta)}{\theta} d\theta\right) \exp\left\{-\left(\int_{t_{i-1}}^{t_i} \frac{d\lambda}{\tau(\lambda)}\right)^{\beta}\right\} \quad (8)$$

T_0 is a reference temperature above the glass transition, and S_c^{eq} is the equilibrium configurational entropy:

$$S_c^{eq}(T) = \int_{T_2}^{T} \frac{\Delta C_p(\theta)}{\theta} d\theta \quad (9)$$

In eq 9, T_2 plays the role of the Kauzmann temperature.[25] In eq 8, the limit configurational heat capacity $\Delta C_p^{lim}(T) = C_p^{lim}(T) - C_{p,glass}(T)$ replaces $\Delta C_p(T)$, so that at temperatures $T < T_g$ $C_p^{lim}(T)$ may assume values different from the ones of the extrapolated heat capacity $C_{p,liq}(T)$. By setting for the completely relaxed configurational entropy $S_c^{lim}(T)$

$$\frac{dS_c^{lim}(T)}{dT} = \frac{\Delta C_p^{lim}(T)}{T} \quad (10)$$

with the condition $S_c^{lim}(T_0) = S_c^{eq}(T_0)$ for $T_0 \gg T_g$, it follows

$$S_c^{lim}(T) = S_c^{eq}(T_0) + \int_{T_0}^{T} \frac{\Delta C_p^{lim}(\theta)}{\theta} d\theta \quad (11)$$

To compute via eq 8 the evolution of configurational entropy during the aging process, an expression for the out of equilibrium relaxation times was proposed,[15] which is a generalization to the nonequilibrium case of the Adam−Gibbs theory.[26]

$$\tau(t) = \tau(S_c(t), T(t)) = A \exp\left(\frac{B}{S_c T}\right) \quad (12)$$

Assuming identical relaxation mechanisms for configurational entropy and enthalpy, one finds

$$H_c(T) = H_c^{lim}(T) - \sum_{i=1}^{n}\left(\int_{T_{i-1}}^{T_i} \Delta C_p^{lim}(\theta)\, d\theta\right) \times \exp\left\{-\left(\int_{t_{i-1}}^{t_i} \frac{d\lambda}{\tau(\lambda)}\right)^{\beta}\right\} \quad (13)$$

This provides the chance of comparing the model with DSC experiments, being the theoretical $C_p(T)$ evaluated from the relation

$$C_p(T) - C_{p,glass}(T) = \frac{\partial H_c}{\partial T} \quad (14)$$

The approach is very similar to the SH model if it is set in eq 8 $C_p^{lim}(T) = C_{p,liq}(T)$. Because information on the temperature dependence of $C_p^{lim}(T)$ is lacking, additional assumptions are necessary. A phenomenological shift of the $C_p^{lim}(T)$ with respect to $C_{p,liq}(T)$ was considered, in a narrow temperature range around the glass transition temperature (see Figure 1),[22] to account for the overestimation of the enthalpy found by the TNM model. In correspondence of the dependence of C_p, in Figure 1 the behavior of the configurational entropy is sketched for the liquid state (equilibrium), for an

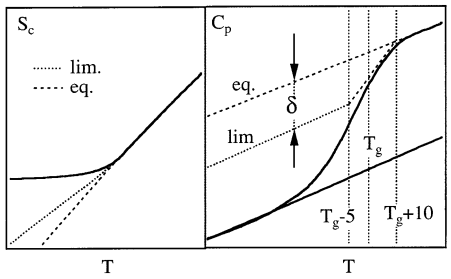

Figure 1. Scheme of the phenomenological parameter δ introduced in ref 22 representing the shift in the limit glassy heat capacity with respect to its extrapolation from the melt (right). On the left, the effects on the configurational entropy are shown.

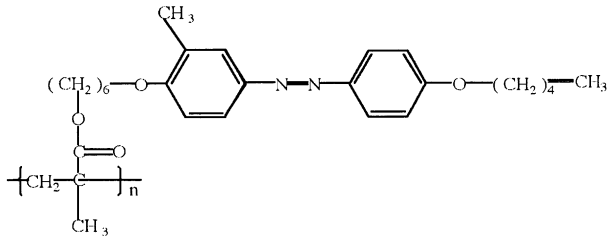

Figure 2. Repeating unit of the polymethacrylate liquid crystal polymer (PMA4) containing the azobenzene mesogenic unit in its side chain.

experimental scan at finite rate (solid line), and for the hypothetical limit of the structural relaxation process. This metastable limit, intermediate between liquid and glass, is distintive of polymers and could originate from a collapse of the configurational rearrangements of the polymer chain when their number reach a limit, probably highly influenced by the presence of topological constraints such as entanglement. Because at the present no information is available on the dependence of S_c on thermal history or annealing temperature, it is assumed the simplest shape for S_c^{lim} (Figure 1), which leads to a constant shift parameter δ for the heat capacity. From the practical point of view, one more free parameter is added to the entropic model.

III. Experimental Section

The polymers under study are side-chain liquid crystal polymethacrylates containing a (3-methyl-4′-pentyloxy) azobenzene mesogenic unit connected at the 4-position by an hexamethylene spacer to the main chain. They were synthesized following a general literature procedure.[27] X-ray measurements confirmed their nematic character in the temperature range between the glass transition T_g and the clearing temperature T_i. The values of T_g were determined according to the enthalpic definition,[28] using a cooling rate of 40 K/min. The homopolymer (thereafter PMA4) has $M_n \approx 19\,000$ Da and $M_w \approx 59\,000$ Da, and its glass transition and clearing temperatures are respectively $T_g = 292$ K and $T_i = 353$ K. Its repeating unit is shown in Figure 2. A random copolymer of PMA4 was prepared by addition of standard MMA monomers with the ratio MA4/MMA = 4; the resulting polymer will be referred to with the acronym PMA80/20. Differences from the homopolymer in the values of temperatures ($T_g \approx 308$ K, $T_i = 348$ K) are according to the expectations. The copolymer exhibits $M_n \approx 8000$ Da and $M_w \approx 31\,000$ Da.

Differential scanning calorimetry measurements were carried out with a Perkin-Elmer DSC 7, frequently calibrated with indium and zinc standards. All thermal treatments were performed without removing the sample from the DSC instrument.

In the experiments, the samples (ca. 10 mg) were (i) first maintained at 388 K, well above T_i, for 15 min in order to erase any previous thermal history; (ii) quenched ($Q_c = 40$ K (min)$^{-1}$) to the temperature $T_a < T_g$ and there annealed for the aging period t_a; and (iii) quenched to a temperature well below the glass transition ($T_g - 70$ K); then a thermogram was recorded on heating at a rate of 10 K min^{-1}.

After each measurement, a reference trace was recorded following the steps i and iii.

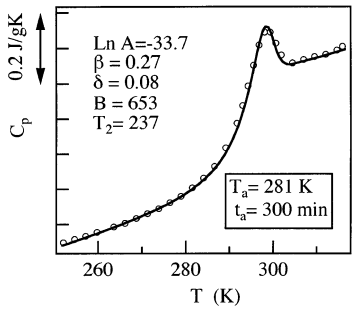

Figure 3. Comparison between the experimental DSC trace of PMA4 recorded after annealing at $T_a = 281$ K for $t_a = 5$ h and the best fit obtained by the entropic model with $T_2 = 237$ K. The other parameters found by the fitting procedure are reported in the figure.

IV. Results and Discussion

To test the entropic approach, the function $\Delta C_p(T)$ (eq 5) has to be determined. This is done by linearly fitting and averaging several thermograms in the proper temperature ranges.

$\Delta C_p(T)$ of PMA4 shows a very weak temperature dependence, and it is found $\Delta C_p(T) = 0.31$ J/(g K) within the experimental errors. The calorimetric trace of the copolymer is characterized by a glass transition interval ending in very proximity of the onset of the clearing peak, which rendered more difficult the determination of a linear expression for $C_p^{liq}(T)$. A weak temperature dependence of ΔC_p is found also for PMA80/20, and the value $\Delta C_p(T) = 0.34$ J/(g K) was taken. It is worthwhile to note that the entropic model results to be quite robust for different choices of the function describing $\Delta C_p(T)$.[29]

A strong correlation is observed between the parameters of the entropic model.[29,30] The procedure keeps constant one of them, while the others are varied to optimize the theory to the experiment. This provides different sets of parameters that can show comparable agreement with experimental data.

In the present paper the Kauzmann temperature T_2, for which some predictions are possible in both polymers[31] and low molecular weight glass formers,[32] is retained as fixed. Numerical optimizations were carried out, with the Nedler−Mead routine,[33] at T_2 constant for PMA4 in the interval 200 K $< T_2 <$ 270 K, while the range 210 K $< T_2 <$ 280 K was spanned for the statistical copolymer PMA80/20.

In Figures 3 and 4, two DSC scans of PMA4, recorded after annealing under quite different conditions, are compared with the best fits with $T_2 = 237$ K. The ability of the model is apparent in reproducing the position and shape of the C_p peaks which signal the enthalpy recovery. More importantly, both experiments exhibit similar best fit parameters, with the greatest variation less than 10%. Very different results[14] were obtained working with the TNM models.

A more severe test of the model is performed by a simultaneous fit of six experimental scans, having different annealing temperatures and different aging

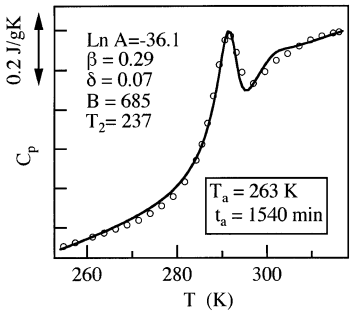

Figure 4. Comparison between the experimental DSC trace of PMA4 recorded after annealing at $T_a = 263$ K for $t_a = 1540$ min and the best fit obtained by setting $T_2 = 237$ K. The values of the other parameters are reported in the figure.

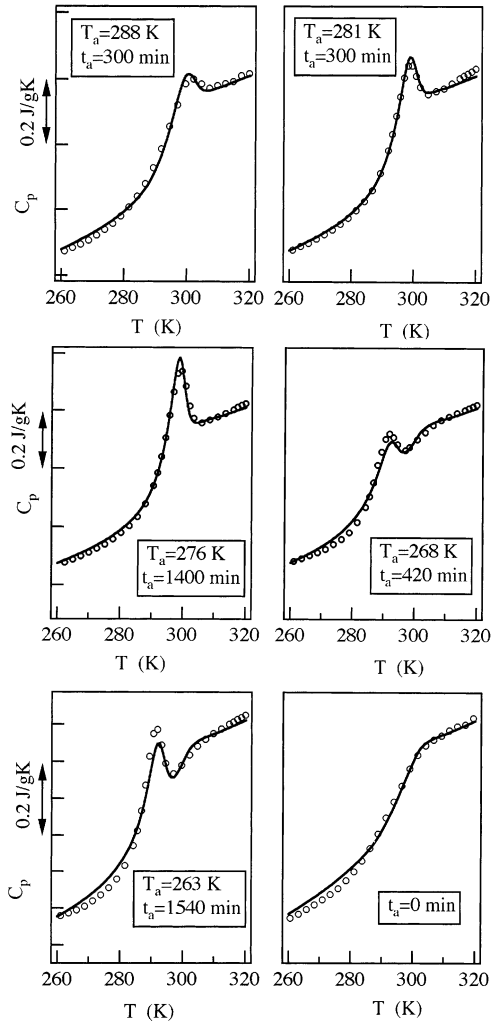

Figure 5. Simultaneous least-squares fit of some DSC traces of PMA4 recorded after different thermal treatments. The aging temperatures and times are reported in the figures. $T_2 = 227$ K; the other parameters are found in Table 1.

times. For PMA4, experimental traces and best fit corresponding to $T_2 = 227$ K are presented in Figure 5. Other fit parameters are reported in Table 1. The figure evidences the agreement between the calculated curves and the PMA4 thermograms. Excluding values of $T_2 >$ 260 K, comparable agreement was obtained for different choices of T_2. Figure 6 compares the experimental traces of PMA80/20 and the simultaneous fit with $T_2 = 247$ K (Table 2). Agreement between experiment and theory was observed, whenever $T_2 < 270$ K.

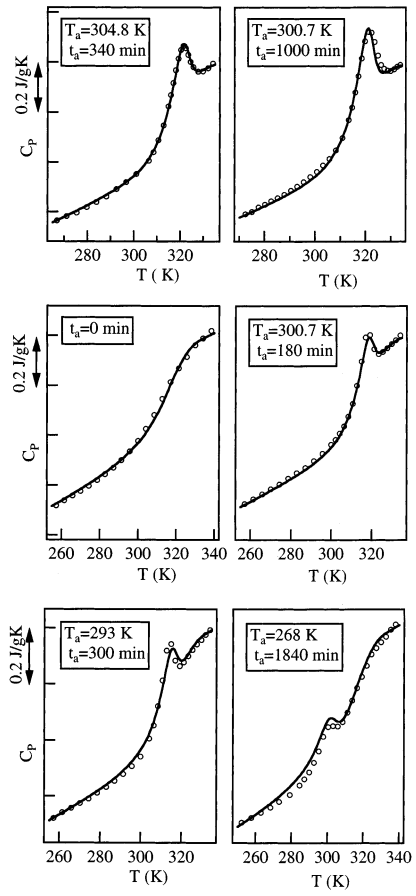

Figure 6. Simultaneous least-squares fit of DSC traces of PMA80/20 recorded after different thermal treatments. The aging temperatures and times are reported in the figures. $T_2 = 247$ K; the other parameters are found in Table 2.

Table 1. Parameters of the Entropic Model in PMA4 for Different Choices of T_2

T_2 (K)	B (J/g)	A (s)	β	δ (J/(g K))	$T_g - T_2$ (K)
227	840.0	1.4×10^{-14}	0.28	0.08	65
237	619.8	8.3×10^{-13}	0.27	0.08	55
242	509.6	1.2×10^{-11}	0.26	0.07	50
252	339.5	1.3×10^{-9}	0.26	0.08	40

Table 2. Parameters of the Entropic Model in PMA80/20 for Different Choices of T_2

T_2 (K)	B (J/g)	A (s)	β	δ (J/(g K))	$T_g - T_2$ (K)
237	1240.0	1.4×10^{-16}	0.24	0.09	70
247	951.0	5.3×10^{-14}	0.23	0.09	60
257	742.0	8.4×10^{-13}	0.23	0.08	50
272	395.3	2.7×10^{-9}	0.23	0.08	35

By inspection of Figures 5 and 6, some features of the materials response after very different thermal treatments are apparent: for annealing well below the glass transition, the C_p peak is concentrated in the transition region, whereas for higher annealing temperatures, it overshoots the end of the glass transition. This trend is accounted for by the evolution of the out of equilibrium configurational entropy evaluated with the entropic model for the heating scan which follows the annealing procedures. Figure 7 shows the PMA4 case: for the lowest annealing temperature $T_a = 263$ K $\approx T_g - 30$ K, S_c exhibits a sharp variation at temperatures well below the glass transition, whereas for the highest annealing temperature, $T_a = 281$ K $\approx T_g - 10$ K, it becomes smaller than its limit value, recovering the equilibrium at temperatures higher than T_g.

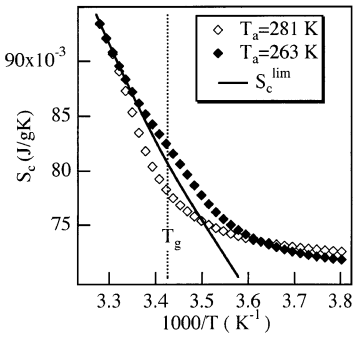

Figure 7. Evolution of the configurational entropy in PMA4 as obtained by the entropic model during the final heating scan after aging at different temperatures. For both examples the annealing time is 5 h. The values of the model parameters are reported in Table 1 (T_2 = 227 K). The full line represents the limit curve of S_c.

The parameters of the simultaneous fits with different T_2 for the same material are found to be different from one set to another (Tables 1 and 2). The biggest variations concern the parameters A and B (see eq 12). This is understood considering that, in the entropic model, the C_p peak of the DSC scans depends on the out of equilibrium behavior of the relaxation times during the measurement on heating. Being the latter mainly determined by the same A, B, and T_2 parameters which provide the equilibrium relaxation times, different choices of T_2 correspond to different values of A and B.

The δ parameter varies in the range 0.07−0.08 J/(g K) for PMA4 and 0.08−0.09 J/(g K) for PMA80/20. These values appear independent of T_2, as usually found in the literature,[22] and substantially independent of the material. This is expected considering the analogous branched structure of PMA4 and random PMA80/20.[30] The above values of δ represent approximately the 25% of the overall C_p changes at the glass transition. Greater values of δ, found in other systems,[30,34] were not expected in the present study, in agreement with our previous work discussing the SH model.[14] In any case, the above amount of the δ shift is sufficient to induce appreciable effects, especially in the predictions about the enthalpy lost by the system during the aging. From the experiments, after annealing at $T_a < T_g$ for an aging time t_a, it may be evaluated according to[35]

$$\Delta H(T_a,t_a) = \int_{T_x}^{T_y}\{C_p^a(T) - C_p^u(T)\}\,dT \qquad (15)$$

$C_p^a(T)$ and $C_p^u(T)$ are the heat capacity after annealing at T_a for the time t_a and the heat capacity of the unannealed sample, respectively; T_x and T_y are reference temperatures such as $T_x < T_g < T_y$. For PMA4 aged at T_a = 281 K, experimental ΔH is compared with the predictions of TNM and entropic models in Figure 8, and in Figure 9 the temperatures corresponding to the maximum of the endothermic peak of the DSC thermograms are reported for the experiment and the entropic model predictions.

Figures 10 and 11 present the analysis for PMA80/20 aged at T_a = 304.7 K.

By inspection of the figures, it is seen that the experiments are well reproduced by the entropic model. The discrepancies regarding the enthalpy loss could be related to the smallness of δ. However, a contribution could originate from the experimental procedure in evaluating $\Delta H(T_a,t_a)$, which underestimates the enthalpy loss.[13] In fact, in eq 15 it is assumed that below T_a the enthalpy curves are parallel during the quench to the temperature well below the glass transition both after annealing (step iii described in the Experimental Section) and for the reference scan. While this approach

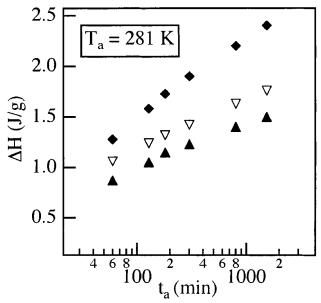

Figure 8. Enthalpy lost due to the aging of the PMA4 sample at T_a = 281 K for different annealing periods: (▲) experimental values evaluated with eq 14; (▽) enthalpy values according to the configurational model (T_2 = 227 K, other parameters in Table 1); (◆) prediction of the TNM model (ref 14).

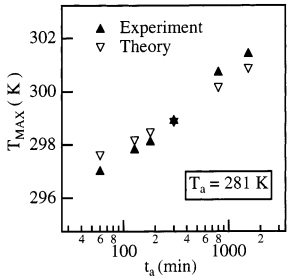

Figure 9. Temperature of the maximum of DSC traces recorded after aging PMA4 sample at 281 K for different t_a. Comparison between the experiment and the prediction of the entropic model (T_2 = 227 K, other parameters in Table 1).

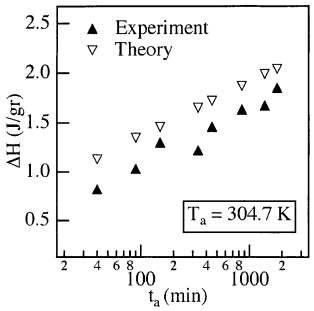

Figure 10. Enthalpy loss after aging PMA80/20 at 304.7 K for different annealing t_a. Comparison between the experiment results, according to eq 14, and the evaluation in terms of the configurational entropy approach (T_2 = 257 K; other parameters in Table 2).

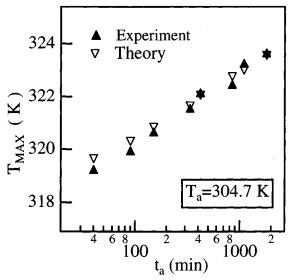

Figure 11. Temperature of the maximum of DSC traces recorded after aging PMA80/20 at 304.7 K for different t_a. Comparison between the experiment and the prediction of the entropic model (T_2 = 257 K; other parameters in Table 2).

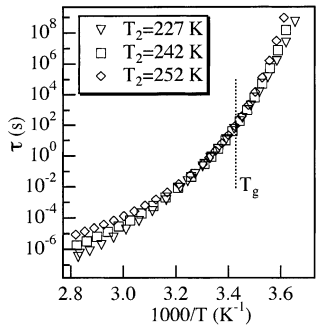

Figure 12. Temperature dependence of the equilibrium structural relaxation times of PMA4, as obtained by the different sets of parameters of Table 1. The coincidence of the different curves around the glass transition is remarkable.

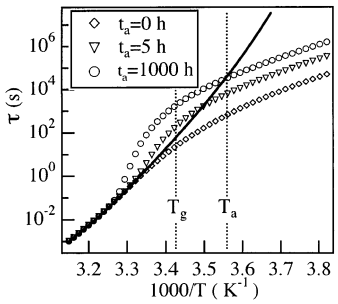

Figure 13. Predictions of the entropic model for the temperature dependence of the out of equilibrium relaxation times during the final heating ramp, after aging procedures at $T =$ 281 K for different annealing times t_a. The values of the parameters are reported in Table 1 ($T_2 = 227$ K).

could be valid after annealing in the deeply glassy state, the experimental case could be very different when the material is annealed at the glass transition. These flaws have been indeed evidenced in this work with numerical calculations.

It was previously remarked that different choices of T_2 within the entropic model bring comparable agreement between theoretical and experimental traces. Even if different, these sets of parameters univocally determine the structural relaxation mechanism of the system. The temperature dependence of the equilibrium relaxation times is obtained by putting in eq 12 the equilibrium configurational entropy S_c^{eq} of eq 9. In Figure 12, the relaxation times of PMA4 for the different sets of parameters of Table 1 are compared. The curves are almost indistinguishable in the narrow temperature range around the glass transition, which is the sole range important in calculating the DSC traces. Similar results were found for PMA80/20.

On discussing the parameters of the tables, the dependence of the DSC peaks on the out-of-equilibrium relaxation times was noted. Their temperature dependence in PMA4, after aging at $T_a = 281$ K for different t_a, is shown in Figure 13 for the set of parameters with $T_2 = 227$ K. The greater the annealing time, the higher the decrement of configurational entropy. Consequently, the relaxation times greatly increase, and the equilibrium recovery takes place at higher temperatures with greater change in a narrow temperature range, as observed experimentally.

From the above results, it can be concluded that the simultaneous fitting procedure is able to determine the equilibrium relaxation times in proximity of the glass transition and, with some uncertainty, the nonexponential parameter β and the shift δ.

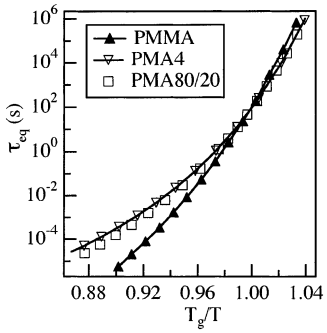

Figure 14. Comparison between the equilibrium enthalpic relaxation times of PMA4, PMA80/20, and PMMA, drawn by analyzing of DSC experiments in terms of the entropic model. The model parameters for PMA4 and PMA80/20 are reported in Tables 1 and 2 ($T_2 = 242$ and 257 K, respectively). Data for PMMA were taken by ref 29.

The values of equilibrium structural relaxation times of the two liquid crystal polymers are interestingly compared by defining a reduced temperature T_g/T (Figure 14). They were calculated by setting $T_g - T_2 =$ 50 K to remove the uncertainty, of the order of 10%, coming from the different set parameters. In the figure the structural relaxation times of the PMMA polymer (full triangles) obtained with the same entropic model[29] are also presented for comparison. The glass transition temperature was set as the temperature corresponding to a structural relaxation time of 100 s; an appreciable change with respect to the enthalpic definition of the glass transition was observed only for the copolymer. By inspection, it is seen that the structural relaxation times show a similar temperature dependence for PMA4 and PMA80/20 and behave differently for PMMA.

Quantitative comparisons may be carried out according to the strong/fragile classification of liquids.[36] The steepness index m

$$m = \frac{\mathrm{d}\log(\tau)}{\mathrm{d}(T_g/T)}\Big|_{T_g} \qquad (16)$$

characterizes the kinetic fragility and, even if criticized,[37] may be used as a general tool in comparing different systems. m varies between 200 and 16 if one ranges from fragile to strong polymers.

It is found $m \approx 80$, 85, and 110 for PMA4, PMA80/20, and PMMA, respectively. From the m values, it seems that the side chains induce a decrease of the steepness index, shifting the response of the liquid crystal polymer toward the strong character.

Interestingly, the viscoelastic structural relaxation times showed a strong/fragile trend similar to that of the enthalpic relaxation. It is seen in Figure 15, where the glass transition temperature was analogously defined by setting $\tau(T_g) = 100$ s.

A physical interpretation of the fragility of the glass formers is still lacking, and several recent studies are devoted to investigate the correlation between dynamic fragility and molecular structure.[36] Literature studies already evidenced that the polymers with longer side chains behave in a stronger way,[29,38] suggesting a relationship with the topological constraints induced by the side chains. Other investigations concern the fragility as measured by different experimental techniques. Recent publications[39] discuss possible correlations between kinetic and thermodynamic fragility, the latter

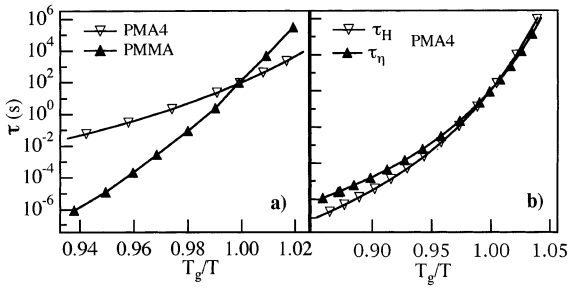

Figure 15. (a) Comparison between the viscoelastic relaxation times of PMA4 and PMMA. (b) Comparison between the viscoelastic and enthalpic relaxation times of PMA4.

defined as the rapidity of the decrease in the configurational entropy as a function of temperature.

In the present work it can be noted that the heat capacity change at the glass transition is greater in the liquid crystal polymers than in PMMA, even if the latter is more fragile in character. This was also observed in many polymeric systems and could suggest either that the correlation[40] between dynamic fragility and heat capacity increment at the glass transition does not hold in polymers[41] or, according to a recent paper,[42] that polymers exhibit negative correlation at the glass transition.

Finally, the nonexponential β parameter is worth some considerations. The values are found of 0.27 and 0.23 for PMA4 and PMA80/20, respectively (Tables 1 and 2). An enthalpy relaxation investigation on PMMA, PEMA, and PBMA[29] provided the values 0.33 ± 0.02, 0.31 ± 0.02, and 0.27 ± 0.02. The β decrement as the side-chain length increases in polymethacrylates seems confirmed.

According to the heterogeneous interpretation of structural relaxation in glass formers,[43] the lower the β value, the broader the distribution of relaxation times. The consequent heterogeneous character of structural relaxation in these polymers is not surprising, considering the intrinsic complexity of their molecular architecture. On the other hand, this highly heterogeneous behavior was already evidenced in PMA4 polymer by means of electron spin resonance studies of the rotational diffusion of a paramagnetic molecular tracer.[6]

As a final remark, the trend observed in the β values in polymethacrylates represents a violation of the inverse correlation between the dynamic fragility m and the nonexponential β parameter, found in glass formers.[44] However, the degree of nonexponentiality drawn with DSC studies could appreciably depart from that obtained with other experimental techniques[45] because of the nonlinear relaxation dynamics probed by DSC experiments and the assumed validity of the time−temperature superposition principle.

V. Conclusions

The structural relaxation of two side-chain liquid crystal polymethacrylates was studied with differential scanning calorimetry. The experimental results were analyzed in terms of a configurational entropic model recently developed. The model was able to describe different DSC traces with a single set of parameters. The simultaneous fitting of different DSC curves provided the temperature dependence of the equilibrium structural relaxation times and the form parameter β. The shift factor δ was also determined, which according to the model fixes the long time limit structural state of the system. However, values of parameters, such as the Kauzmann temperature T_2 and the activation pseudoenergy B, were not unambiguously determined by the model.

The introduction of a reduced temperature (T_g/T) allowed the comparison of the equilibrium relaxation times of the two polymers with the standard poly(methyl methacrylate) analyzed in terms of same model. The liquid crystal polymers were found to behave in a similar way, evidencing a stronger character than PMMA, according to strong/fragile classification. The same trend was found for relaxation times of the shear flow. This result seems to confirm the connection between fragility and the length of the side groups of the polymeric backbone. Finally, the β parameter evidenced the great dynamical heterogeneity of these LC polymer.

Acknowledgment. This work is supported by the MIUR and INFM (CIPE Project P5BW5). We are grateful to G. Galli and M. Laus for providing the new synthesized PMA4 and PMA80/20.

References and Notes

(1) McArdle, C. B. In *Side Chain Liquid Crystal Polymers*; McArdle C. B., Ed.; Blakie and Son Ltd: Glasgow, 1989.
(2) Eich, M.; Wendorff, J. H. *Makromol. Chem. Rapid Commun.* **1987**, *8*, 59. Eich, M.; Wendorff, J. H. *Makromol. Chem. Rapid Commun.* **1987**, *8*, 467.
(3) Andreozzi, L.; Camorani, P.; Faetti, M.; Palazzuoli, D. *Mol. Cryst. Liq. Cryst.* **2001**, *375*, 129. Patanè, S.; Arena, A.; Allegrini, M.; Andreozzi, L.; Faetti, M.; Giordano, M. *Opt. Commun.* **2002**, *210*, 37.
(4) Ikeda, T.; Wu, Y. *Pure Appl. Chem.* **1999**, *71*, 2131.
(5) Bubliz, D.; Helgert, M.; Fleck, B.; Wenke, L.; Hvilsted, S.; Ramanujam, P. S. *Appl. Phys. B: Laser Opt.* **2000**, *70*, 803. Helgert, M.; Fleck, B.; Wenke, L.; Hvilsted, S.; Ramanujam, P. S. *Appl. Phys. B: Laser Opt.* **2000**, *70*, 863.
(6) Andreozzi, L.; Faetti, M.; Galli, G.; Giordano, M.; Palazzuoli, D. *Macromolecules* **2001**, *34*, 7325.
(7) Hodge, I. M. *J. Non-Cryst. Solids* **1994**, *169*, 211.
(8) Hutchinson, J. M. *Prog. Polym. Sci.* **1995**, *20*, 703.
(9) Tool, A. Q. *J. Am. Ceram. Soc.* **1946**, *29*, 240.
(10) Narayanaswamy, O. S. *J. Am. Ceram. Soc.* **1971**, *54*, 491. Moynihan, C. T.; Easteal, A. J.; DeBolt, M. A.; Tucker, J. *J. Am. Ceram. Soc.* **1976**, *59*, 12.
(11) Tribone, J. J.; O'Reilly, J. M.; Greener, J. *Macromolecules* **1986**, *19*, 1732.
(12) Cowie, J. M. G.; Ferguson, R. *Polymer* **1993**, *34*, 2135.
(13) Gómez Ribelles, J. L.; Ribes Greus, A.; Diaz Calleja, R. *Polymer* **1990**, *31*, 223.
(14) Andreozzi, L.; Faetti, M.; Giordano, M.; Palazzuoli, D. *Philos. Mag. B* **2002**, *82*, 397.
(15) Gómez Ribelles, J. L.; Monleón Pradas, M. *Macromolecules* **1995**, *28*, 5867.
(16) Phillips, J. C. *Rep. Prog. Phys.* **1996**, *59*, 1133.
(17) Hodge, I. M.; Berens A. R. *Macromolecules* **1982**, *15*, 762.
(18) Moynihan, C. T.; Macedo, P. B.; Montrose, C. J.; Gupta, P. K.; DeBolt, M. A.; Dill, J. F.; Dom, B. E.; Drake, P. W.; Easteal, A. J.; Elterman, P. B.; Moeller, R. P.; Sasabe, H.; Wilder, J. A. *Ann. N.Y. Acad. Sci.* **1976**, *279*, 15.
(19) Sherer, G. W. *J. Am. Ceram. Soc.* **1984**, *67*, 504. Hodge, I. M. *Macromolecules* **1987**, *20*, 2897.
(20) Hodge, I. M. *J. Res. Natl. Inst. Stand. Technol.* **1997**, *102*, 195.
(21) Mano, J. F.; Alves, N. M.; Meseguer Dueñas, J. M.; Gómez Ribelles, J. L. *Polymer* **1999**, *40*, 6545.
(22) Meseguer Dueñas, J. M.; Garayo, A. V.; Romero Colomer, F.; Estellés, J. M.; Gómez Ribelles, J. L.; Monleón Pradas, M. *J. Polym. Sci., Part B: Polym. Phys.* **1997**, *35*, 2201.
(23) Mascarell, J. B.; Belmonte, G. G. *J. Chem. Phys.* **2000**, *113*, 4965.
(24) Simon, S. L. *Macromolecules* **1997**, *30*, 4056. Hodge, I. M. *J. Non-Cryst. Solids* **1991**, *131−133*, 435.
(25) Kauzmann, W. *Chem. Rev.* **1948**, *43*, 219.
(26) Adam, G.; Gibbs, J. H. *J. Chem. Phys.* **1965**, *43*, 139.

(27) Angeloni, A. S.; Caretti, D.; Laus, M.; Chiellini, E.; Galli, G. *J. Polym. Sci., Polym. Chem. Ed.* **1991**, *29*, 1865.
(28) Richardson, M. J.; Savill, N. G. *Polymer* **1975**, *16*, 753.
(29) Gómez Ribelles, J. L.; Monleón Pradas, M.; Garayo, A. V.; Romero Colomer, F.; Estellés, J. M.; Meseguer Dueñas, J. M. *Macromolecules* **1995**, *28*, 5878.
(30) Gómez Ribelles, J. L.; Monleón Pradas, M.; Meseguer Dueñas, J. M.; Privalko, V. P. *J. Non-Cryst. Solids* **1999**, *244*, 172.
(31) Ferry, J. D. *Viscoelastic Properties of Polymers*, 3rd ed.; Wiley: New York, 1980.
(32) Moynihan, C. T.; Angell, C. A. *J. Non-Cryst. Solids* **2000**, *274*, 131.
(33) Nedler, J. A.; Mead, R. *Comput. J.* **1965**, *7*, 308.
(34) Gómez Ribelles, J. L.; Monleón Pradas, M.; Garayo, A. V.; Romero Colomer, F.; Estellés, J. M.; Meseguer Dueñas, J. M. *Polymer* **1997**, *38*, 963.
(35) Cowie, J. M. G.; Ferguson, R. *Macromolecules* **1989**, *22*, 2307.
(36) Böhmer, R.; Angell, C. A. *Phys. Rev. B* **1992**, *45*, 10091.
(37) Green, J. L.; Ito, K.; Xu, K.; Angell, C. A. *J. Phys. Chem. B* **1999**, *103*, 3991.
(38) Godard, M. E.; Saiter, J. M. *J. Non-Cryst. Solids* **1998**, *235−237*, 635. Hempel, E.; Kahle, S.; Unger, R.; Donth, E. *Thermochim. Acta* **1999**, *329*, 97.
(39) Ito, K.; Moynihan, C. T.; Angell, C. A. *Nature (London)* **1999**, *398*, 492. Ngai, K. L.; Yamamuro, O. *J. Chem. Phys.* **1999**, *111*, 10403.
(40) Angell C. A. *J. Non-Cryst. Solids* **1991**, *131−133*, 13. Angell, C. A. *Science* **1995**, *267*, 1924.
(41) Roland, C. M.; Santangelo, P. G.; Ngai, K. L. *J. Chem. Phys.* **1999**, *111*, 5593.
(42) Huang, D.; McKenna, G. B. *J. Chem. Phys.* **2001**, *114*, 5621.
(43) Sillescu, H. *J. Non-Cryst. Solids* **1999**, *243*, 81.
(44) Böhmer, R.; Ngai, K. L.; Angell, C. A.; Plazek, D. J. *J. Chem. Phys.* **1993**, *99*, 4201.
(45) Moynihan, C. T.; Crichton, S. N.; Opalka, S. M. *J. Non-Cryst. Solids* **1991**, *131−133*, 420.

MA020602Y